The Journal of Neuroscience, July 15, 2002, 22(14):6186–6194

Dendroarchitecture of Relay Cells in Thalamic Barreloids: A Substrate for Cross-Whisker Modulation

Caroline Varga, Attila Sík, Philippe Lavallée, and Martin Deschênes

Centre de Recherche, Université Laval-Robert Giffard, Québec G1J 2G3, Canada

A double-labeling protocol was used to determine how the dendroarchitecture of relay cells relates to the three-dimensional structure of barreloids in the ventral posterior medial nucleus of the rat thalamus. Single barreloids were retrogradely labeled by injecting Fluoro-Gold in identified barrel columns, and single relay cells activated by the same whisker, or by an adjacent whisker located on the same arc, were juxtacellularly labeled with biotinylated dextran. Results show that the dendritic field of relay cells is asymmetric, variously oriented with respect to the geometry of the barreloids, and that all cells extend dendrites in surrounding barreloids. Extrabarreloid dendrites are of small size (<1.5 μm) and represent up to 54% (range, 11–54%) of the total dendritic length. In contrast, the thick proximal dendrites remain confined to the home barreloid of the cell, being directed toward its center or along its margin. There is a trend for cells located dorsally in barreloids to form more elaborate trees with a larger proportion of extrabarreloid dendrites. Electron microscopic examination of labeled cells shows that extrabarreloid dendrites are exclusively contacted by synaptic terminals of cortical and reticular thalamic origin, whereas intrabarreloid dendrites also receive contacts from lemniscal terminals. Because corticothalamic and reticular thalamic cells establish point-to-point connections with homotopic barreloids, it is proposed that the spatial arrangement of dendrites determines the combination of whisker deflection that best modulates cell firing. Because relay cell responses are direction sensitive, maximal modulation would occur if dendritic field orientation relates to the direction selectivity of responses.

Key words: barrels; barreloids; whisker; vibrissa; ventral posterior medial nucleus; thalamic relay cells

The way nerve cells distribute dendrites in laminated structures or in other types of histochemically defined compartments in the brain is one of the factors that determines input selection and integrative properties. In this regard, the vibrissal sensory system of rodents presents itself as a remarkable model of modular organization. From periphery to cortex, this system is made up of discrete cellular aggregates that replicate the arrangement of the vibrissae on the mystacial pad. In the ventral posterior medial (VPM) nucleus of the thalamus, whisker-related modules are called barreloids (Van der Loos, 1976), and each barreloid pairs with a corresponding module, called a barrel, in the primary somatosensory cortex (Woolsey and Van der Loos, 1970). Although barrels are readily outlined by cytochrome oxidase (CO) histochemistry, thalamic barreloids are more difficult to recognize, because their curved three-dimensional structure does not honor section planes commonly used in histological preparations (Land et al., 1995). Because of this limitation, little information is currently available on the relationships between the dendroarchitecture of relay cells and the structure of barreloids, especially in adult rodents. Previous studies have shown that VPM cells have dendritic fields that are more extensive than the average dimension of a barreloid (Harris, 1986; Chiaia et al., 1991; Ohara and Havton, 1994; Zantua et al., 1996), and that trigeminothalamic, corticothalamic, and reticular thalamic axons form in VPM terminal fields that are restricted to the dimension of a single barreloid (Williams et al., 1994; Bourassa et al., 1995; Cox et al., 1996; Veinante and Deschênes, 1999; Désîlets-Roy et al., 2002). Thus, the way relay cells distribute dendrites within and across barreloids should be an important factor that determines cross-whisker integrative properties. In the present study, we used a double-labeling protocol to establish how the dendroarchitecture of VPM cells relates to the three-dimensional structure of their home barreloids.

Received Feb. 26, 2002; revised April 22, 2002; accepted April 23, 2002.

This work was supported by Grant MT-5877 from the Canadian Institutes of Health Research (M.D.) and by a Conseil de la Recherche en Sciences Naturelles et Génie du Canada studentship (C.V.). A.S. is a Le Fonds de la Recherche en Santé de Québec scholar. We are grateful to Orsolya Szalay for her efficient technical help.

Correspondence should be addressed to Dr. Martin Deschênes, Centre de Recherche, Université Laval-Robert Giffard, 2601 de la Canardière, Québec G1J 2G3, Canada. E-mail: martind@globetrotter.net.

MATERIALS AND METHODS

Double labeling protocol. Experiments were made in 35 adult rats (Sprague Dawley, 250–300 gm) in accordance with federally prescribed animal care and use guidelines. The University Committee for Animal Use in Research approved all experimental protocols. First, rats were anesthetized with a mixture of ketamine (75 mg/kg) plus xylazine (5 mg/kg), and a barrel column, usually in the C or D rows, was located by recording unit responses to manual whisker deflection. Next, a micropipette (tip diameter, ~6 μm) containing Fluoro-Gold (FG; 2% in 0.1 M cacodylate buffer, pH 7.0; Fluorochrome Inc., Denver, CO) was lowered in layer 4 (depth, 740 μm) of the identified barrel column. The tracer was ejected with positive current pulses of 100 nA for 10 min. After completing this protocol in both hemispheres the skin was sutured; rats were given analgesics (Anafen, 5 mg/kg) and were returned to the animal facilities. After 24–48 hr, animals were reanesthetized with ketamine/xylazine, and we searched for VPM cells that responded to the whisker whose barreloid had been retrogradely labeled with FG. Extracellular recordings were made with fine micropipettes (diameter, 0.5–1 μm) filled with K-acetate (0.5 M) and low molecular mass biotinylated dextran (2% BDA, 3 kDa; Molecular Probes, Eugene, OR). Throughout the experiments a deep level of anesthesia was maintained so that cells only responded to the deflection of one whisker. Once a responsive unit had been isolated, it was juxtacellularly labeled by the application of positive current pulses (2–8 nA; 200 msec durarion; 50% duty cycle) for ~10 min (Pinault, 1996). At the end of the experiments, rats were perfused under deep anesthesia with saline followed by a fixative containing 4% paraformaldehyde and 0.5% glutaraldehyde in phosphate buffer (PB; 0.1 M,

pH 7.4). Brains were removed, postfixed overnight in the same fixative, and cut coronally ($n = 24$) or horizontally ($n = 4$) at 70 μm with a vibratome.

After three washes in PBS (0.01 M, pH 7.4), sections were treated for 30 min with a solution of 50% ethanol plus 1% hydrogen peroxide. They were rinsed several times in PBS and preincubated for 1 hr in PBS with 3% normal goat serum and 0.3% Triton X-100. Then they were incubated overnight in the same medium containing an anti-FG antiserum (1:8000; Chemicon, Temecula, CA). The antibody was revealed using a peroxidase-labeled secondary antibody (goat IgG; Chemicon) and 3,3′-diaminobenzidine tetrahydrochloride (DAB) as a substrate (brown reaction product). Next, sections were processed for BDA histochemistry using the ABC kit (Vector Laboratories, Burlingame, CA) and nickel-DAB (black reaction product). Finally, sections were mounted on gelatin-coated slides, dehydrated in alcohols, cleared in toluene, and coverslipped without counterstaining.

Additional material for morphometric analysis was obtained from previous experiments in which VPM cells had been labeled with BDA, and the tissue was processed for CO histochemistry.

Iontophoresis of lipophylic dyes. In three rats, separate injections of lipophylic dyes [1,1′-dioctadecyl-3,3,3′,3′tetramethylindocarbocyanine perchlorate (DiI) and 4-(4-(dihexadecylamino)styryl)-*N*-methylpyridinium iodide (DiA); Molecular Probes] were made in physiologically identified adjacent barrel columns. Dyes were ejected by iontophoresis to minimize their diffusion to the supragranular layers over the barrels. Micropipettes (tip diameter, ~15 μm) were filled with a dye solution (2% in methylene chloride), and the tracers were ejected by positive current pulses (100 nA; 2 sec duration; half-duty cycle) for 10 min. Dyes were cotransported with methylene ions and crystallized around the tip of the micropipette because of their low water solubility. Rats were perfused after a survival period of 5 d, and brain sections were examined under fluorescent microscopy.

Cell reconstruction and morphometric analysis. Labeled material was drawn at 100× with a camera lucida. After being reconstructed from serial sections by this method, neurons were also reconstructed with the aid of a computer system (Neurolucida; Microbrightfield Inc., Colchester, VT). Arrays of retrogradely labeled cells were outlined by convex contours that were smoothed and connected to generate a solid picture of the barreloids. Morphometric analysis and three-dimensional reconstructions were made with the NeuroExplorer software equipped with the Solid Rendering module (Microbrightfield Inc.). The length of dendrites was measured after correction for shrinkage in the *z*-axis. The shrinkage factor was determined by computing the ratio of section thickness used for tissue sectioning to that measured on slides with the *z*-axis of the microscope stage. No correction was introduced for measurements along the *x*- and *y*-axis, because shrinkage along these dimensions was minimal (<10%) and did not modify the topographic relationship between barreloids and cell architecture. Photomicrographs were taken with a Spot RT camera (Diagnostic Instruments Inc., Sterling Heights, MI) and imported in Photoshop 5.5 (Adobe Systems Inc., San Jose, CA) for contrast and brightness adjustments.

Electron microscopy. In two experiments we combined light and electron microscopic (EM) examination of labeled cells. Surgery and experimental procedures were performed as described above with the following modifications. A cholera toxin b subunit Alexa Fluor 488 conjugate

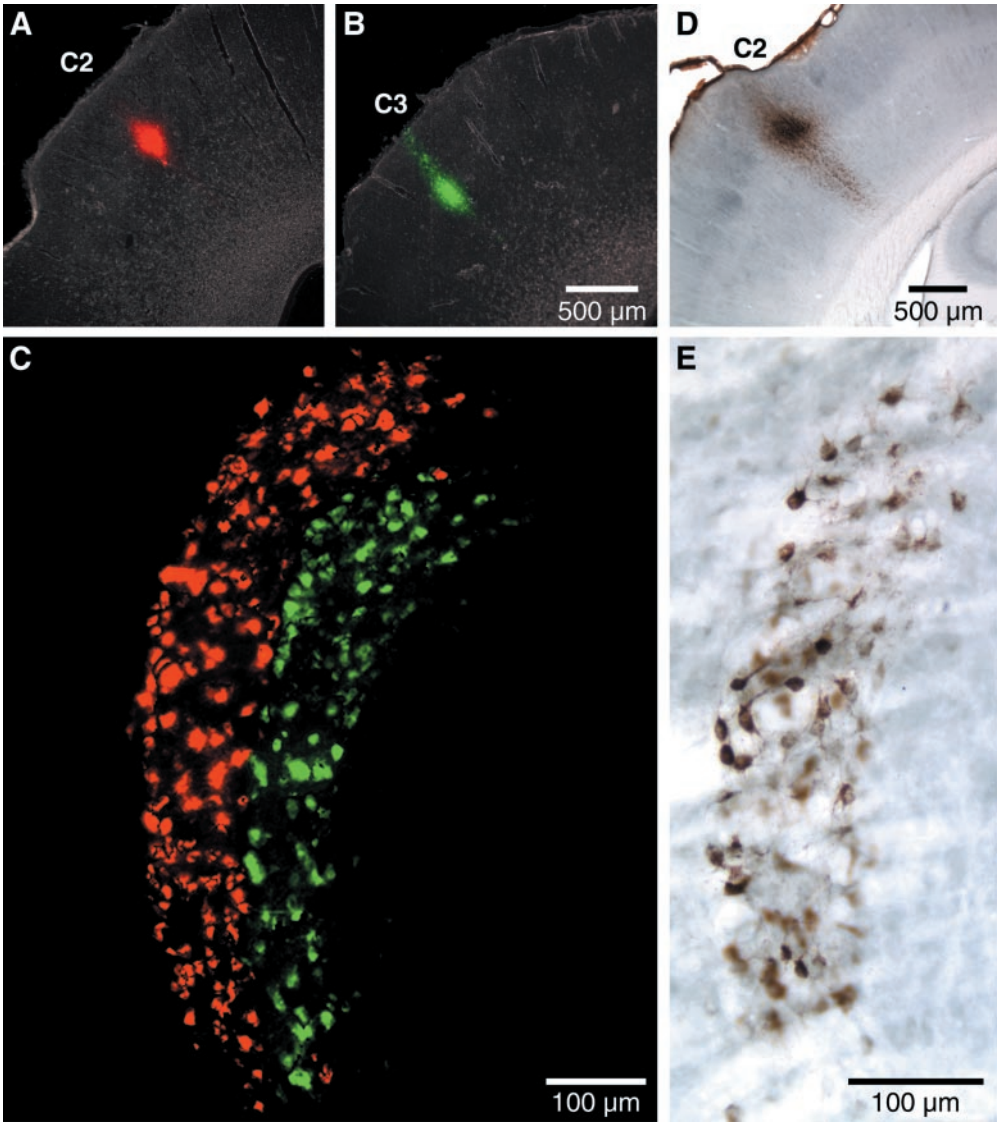

Figure 1. Retrograde labeling of barreloids in the rat VPM. Iontophoretic injections of DiI (*A*) and DiA (*B*) in barrel columns C2 and C3 led to the retrograde labeling of homotopic barreloids (*C*). The photomicrograph in *C* is a montage made from a stack of five consecutive coronal sections. *E* shows retrogradely labeled cells in barreloid C2 after iontophoretic injection of FG in barrel column C2 (*D*).

Table 1. Dendritic length of barreloid cells

Cell (n = 26)	Barreloid	Total dendritic length (μm)	Total length of extrabarreloid dendrites	
			μm	%
1[a]	A1	12,042.1		
2[a]	A2	9,204.2		
3[a]	A4	9,923.6		
4	B2	10,396.0	2705.0	26.0
5	B3	7,155.3	3840.2	53.7
6	C1	6,611.4	747.1	11.3
7	C1	8,214.4	1769.7	21.5
8	C1	10,631.9	5173.6	48.7
9[b]	C1	5,778.3		
10[b]	C1	7,828.2		
11[b]	C1	11,054.0		
12[a]	C2	15,609.3		
13	C2	9,221.8	1322.6	14.3
14	C2	10,187.8	2728.5	26.8
15	C2	13,391.5	5932.8	44.0
16	C2	16,060.6	6466.4	40.3
17	C3	12,553.9	3401.2	27.1
18[b]	C3	11,043.9		
19[a]	C3	11,297.5		
20	C4	8,372.0		
21[a]	C6	17,295.1		
22	D2	12,055.7	6276.0	52.1
23	D2	13,925.7	5070.7	36.0
24[a]	D4	15,423.7		
25[a]	E4	7,751.2		
26[a]	E4	9,805.0		

[a]Cells labeled in CO-stained sections.

[b]Cells labeled next to a backfilled barreloid.

(Molecular Probes) was used to backfill the barreloids. A small volume of tracer (80 nl) was pressure injected in identified barrel columns, and cells were juxtacellularly labeled with BDA 2 d later. Rats were perfused, brains were cut coronally at 60 μm with a vibratome, and the tissue was permeabilized by freeze thawing over liquid nitrogen. BDA was revealed with a streptavidin Alexa Fluor 568 conjugate (Molecular Probes), and labeled material was photographed at several focal planes. Sections were then processed with an ABC kit (Vector Laboratories) and DAB. After osmication (1% osmium tetroxide in PB) for 30 min, sections were washed in PB, dehydrated in a graded series of ethanol, cleared in propylene oxide, and flat embedded in Durcupan. Cells were drawn with a camera lucida at 100×, and drawings were rescaled and overlain on photomicrographs taken under fluorescent microscopy to identify dendrite location with respect to the structure of the labeled barreloid. Thin sections were serially cut on an ultramicrotome, collected on formvar-coated single-slot grids, stained with lead citrate and uranyl acetate, and examined with a Philips (Eindhoven, The Netherlands) Tecnai 12 electron microscope equipped with a Megaview II digital camera (SIS, Germany).

RESULTS

Retrograde labeling defines barreloid boundaries

In CO-stained tissue, barreloids appear as darkly reactive, curved, tapering rods that extend through the thickness of the VPM (Land et al., 1995; Haidarliu and Ahissar, 2001). Their structure is most readily appreciated in sections cut in an oblique sagittal plane, whereas their patterning and identification are better revealed in oblique horizontal sections. An alternative and more convenient way to outline the structure of barreloids is through retrograde labeling. Provided that tracer injections are confined within the limit of a single barrel column, the pattern of retrograde labeling in the VPM precisely matches the shape and dimension of the barreloids seen in CO-stained sections (Hoogland et al., 1987; Land et al., 1995). The sharpest delineation of the barreloids is obtained by iontophoretic injections of lipophylic dyes that diffuse little in tissue. Figure 1*A–C* shows how sharply two barreloids can be defined after separate injections of DiI and DiA in adjacent barrel columns. A similar degree of

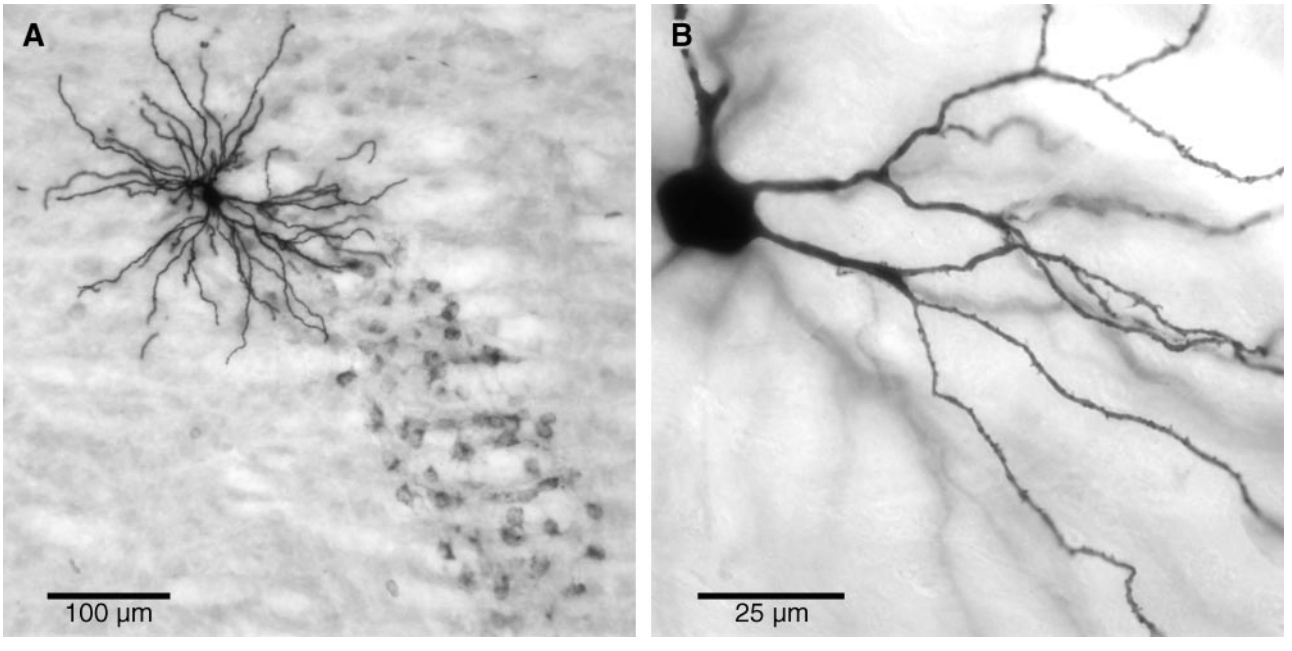

Figure 2. Juxtacellularly stained relay cells in thalamic barreloids. *A*, Barreloid D2 was backfilled with FG and a cell with principal-whisker receptive field on whisker D2 was labeled with BDA. *B*, Aspect of proximal and distal dendrites of a D3-responsive relay cell after osmication and plastic embedding. Note the large number of protrusions on distal dendrites. The cell in *B* was injected with BDA and sections were permeabilized by freeze-thawing over liquid nitrogen.

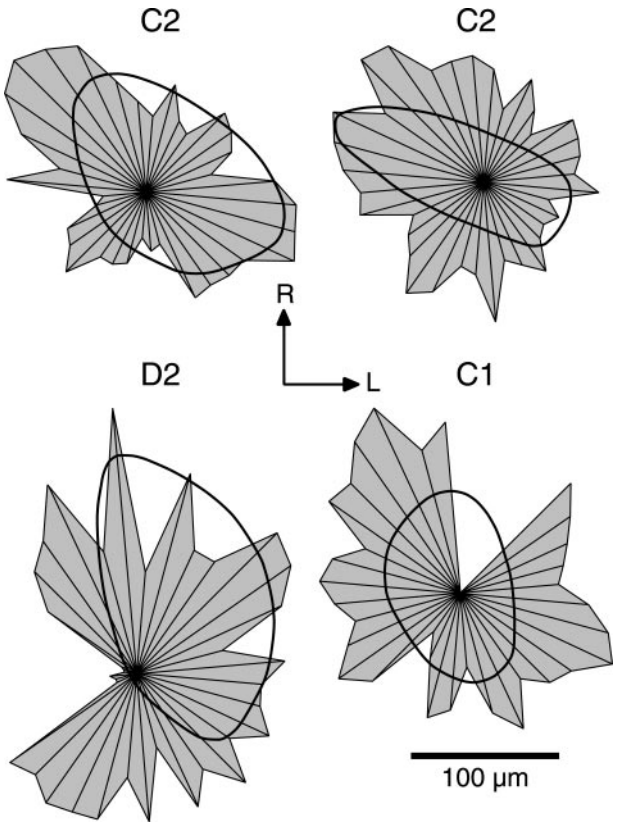

Figure 3. Polar plots showing horizontal projections of the dendritic arbors in 10° segments centered on the cell body for four VPM cells. Superimposed contours outline the cross-section geometry of the barreloids at the level of the cell bodies (barreloids are identified above drawings). *R*, Rostral; *L*, Lateral.

Figure 4. Intrabarreloid distribution of the thick proximal dendrites of relay cells. The proximal dendrites of eight cells responsive to the C1, C2, or D2 whiskers were reconstructed after juxtacellular staining with BDA. Cells were placed in a "reference" barreloid (here, barreloid C2 outlined in *gray*), according to their actual location and orientation in their respective barreloid. Note that thick dendrites do not cross barreloid boundaries.

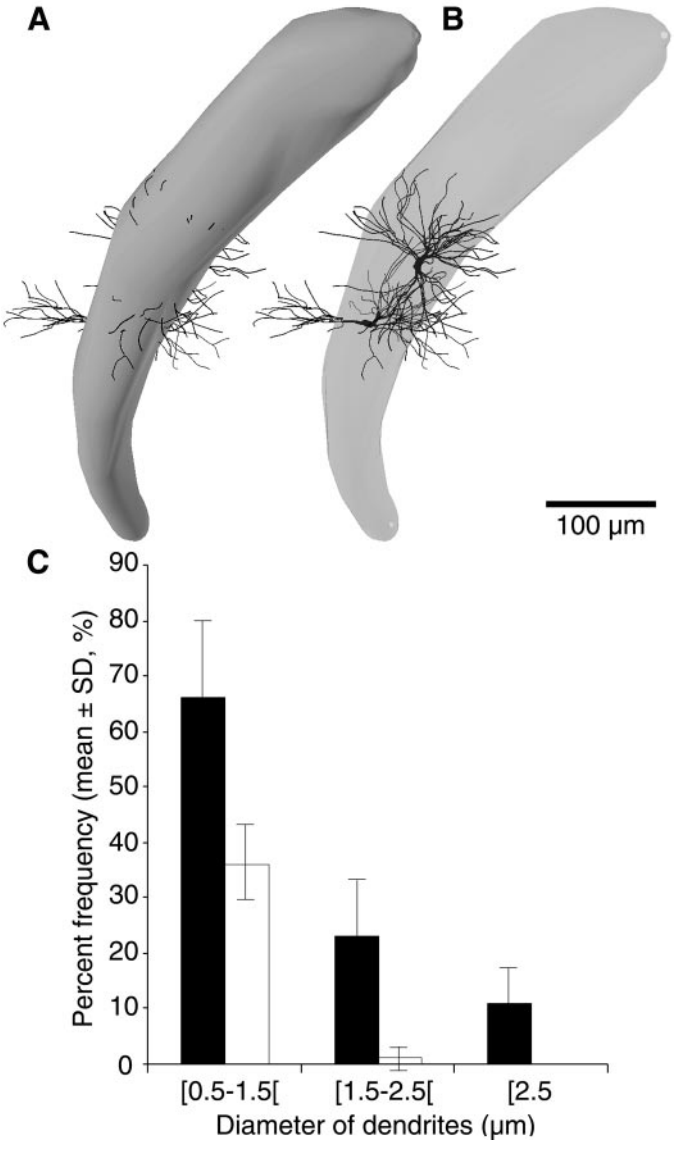

Figure 5. Dendritic arborization of relay cells in surrounding barreloids. Barreloid C2 was retrogradely labeled with FG, and two cells were juxtacellularly stained with BDA. Renderings with and without transparency (*A, B*) highlight the intrabarreloid and extrabarreloid distributions of dendrites. The histogram in *C* shows the distributions of branch diameters for dendrites located inside (*black bars*) and outside (*white bars*) the barreloids. Percentage values in histograms represent means ± SD for a sample of 12 cells.

definition can be obtained with tracers of moderate water solubility, such as FG, by careful control of their application (see Materials and Methods). Injections of the size shown in Figure 1*D* lead to the retrograde labeling of single barreloids in ~50% of cases (Fig. 1*E*). When two barreloids are backfilled, one usually contains less darkly stained somata, so that the border between the two arrays remains clearly discernible. Ambiguous cases of multiple labeling are unavoidable, and these were removed from the present study.

Database

Our database comprises 24 juxtacellularly stained whisker-responsive relay cells (Table 1). Twelve cells were located in the retrogradely filled barreloid, and five were located in an adjacent

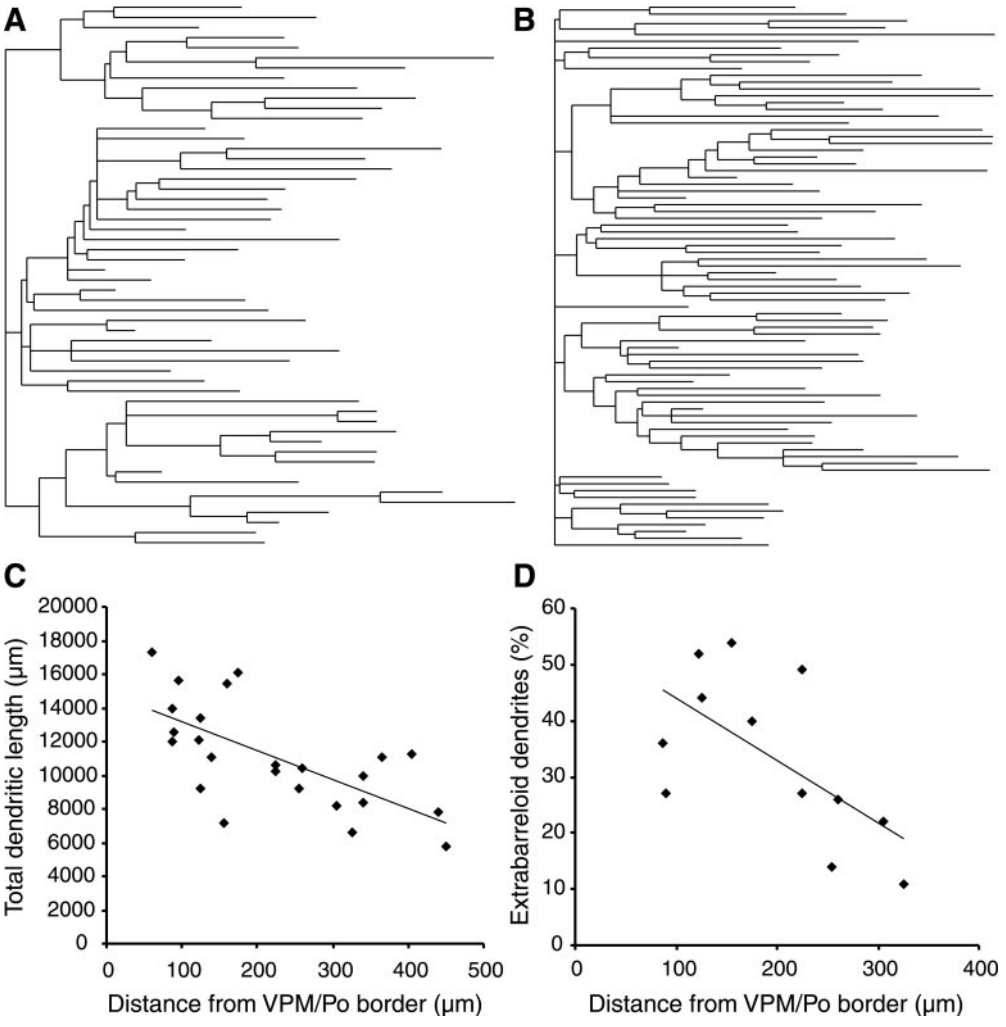

Figure 6. Architecture of the dendritic arbors of VPM relay cells. Dendrograms *A* and *B* show the branching patterns of two cells located in barreloid C2 (cells numbered 13 and 16, respectively, in Table 1). Cell 13 was located at a distance of 250 μm from the VPM/Po border, and its dendrogram contains 54 end points. Cell 16 was located at a distance of 175 μm from the VPM/Po border, and its dendrogram contains 80 end points. The *bottom graphs* show how the total dendritic lengths (*C*) and the percentages of extrabarreloid dendrites (*D*) vary with the distance of cell bodies from the VPM/Po border. This was estimated by drawing the shortest line between both points. Correlation coefficients and regression lines: *C*, $r = -0.68$, $p < 0.001$, and $y = -17.07x + 14{,}842$; *D*, $r = -0.63$, $p < 0.05$, and $y = -0.11 + 55.33$.

barreloid. In all cases cell location was consistent with the electrophysiological identification. The rest of the sample consists of BDA-stained cells in CO-stained sections. Figure 2 shows a representative case of double labeling that combines the backfilling of barreloid D2 with the juxtacellular staining of a D2-responsive relay cell.

Morphology of barreloid cells

Barreloid cells have medium-sized somata (~18 μm) from which emerge four to six thick dendrites (2–4 μm). Within 15–40 μm from the cell body, most primary dendrites divide into bundles of secondary branches (1–2 μm) that form bush-like dendritic trees (Fig. 2). Each tree consists of secondary and higher-order branches that spread out over a distance of 80–125 μm. Distal dendrites exhibit little tapering and often adopt a curved recurrent path before ending. Dendrites bear few pedunculated spines but are covered with a number of small protrusions that give them a rough aspect (Fig. 2*B*). Spines and protrusions are barely discernible in sections permeabilized with Triton X-100 but clearly show up in plastic embedded material prepared for electron microscopy.

Relay cell dendrites extend in surrounding barreloids

Regardless of their localization in a barreloid, the orientations of the dendritic arbors of VPM cells are quite variable. Dendritic fields are often asymmetric, with zones of high branch density and other zones that are almost branch free. The polar graphs of Figure 3 show four projections of dendritic field geometry in the horizontal plane. One can note the asymmetric distribution of dendritic trees around cell bodies, their variable orientation with respect to the anteroposterior and mediolateral axis of the barreloids, and the spread of dendrites in adjacent barreloids.

As a rule, the thick proximal dendrites of relay cells are always confined to their home barreloid. Labeled neurons whose somata lie near the edge of the barreloid have primary dendrites directed toward its center or along its margin. Figure 4 shows the proximal dendritic trunks of eight cells that are localized in different sectors of the C1, C2, or D2 barreloids. Higher-order dendrites that stem from proximal trunks extend both within and outside the barreloid. This feature is clearly highlighted in the solid renderings of Figure 5. Extrabarreloid dendrites are of small size (<1.5 μm) (Fig. 5*C*) and represent up to 54% (range, 11–54%) of the total dendritic length (Table 1). The surface areas of extrabarreloid dendrites represent 19.8–48.8% of the total dendritic surface areas of the cells (range, 21,001–56,237 μm^2).

Total dendritic length and percentage of extrabarreloid dendrites relate to cell location

Although barreloid cells display dendritic fields of approximately the same size (maximal dendritic span, ~250 μm), the total dendritic length generated by individual cells varies over a wide

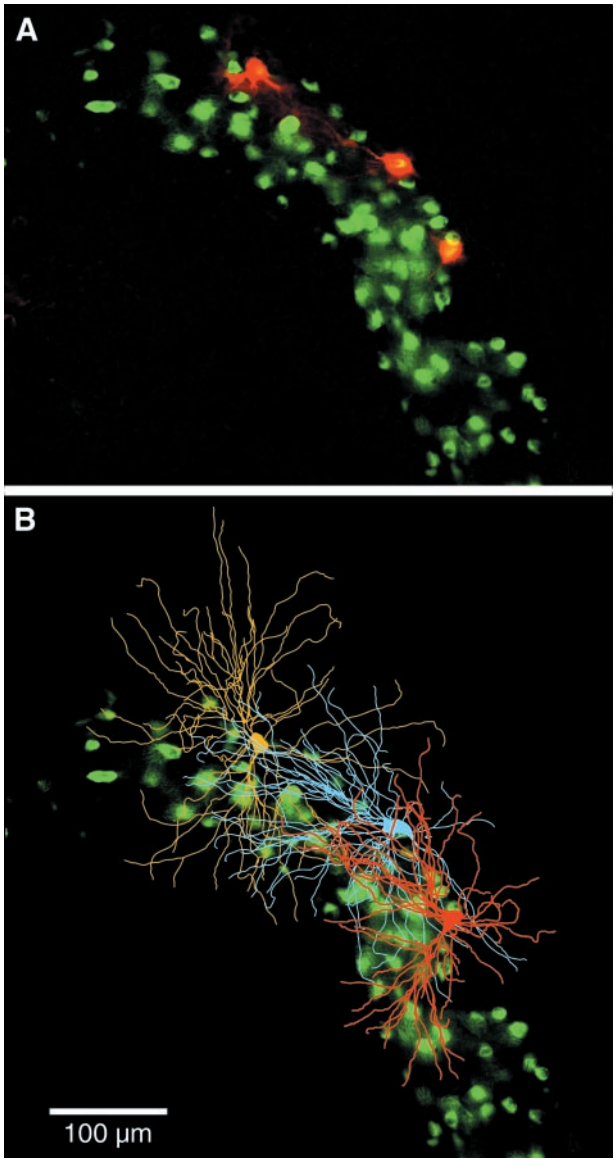

Figure 7. Material used to examine the distribution of synaptic contacts on the dendrites of relay cells. *A*, Double exposure photomicrograph of three cells juxtacellularly stained with BDA in barreloid C2. The barreloid was backfilled with cholera toxin (*green*), and cells were revealed with a *red* fluorescent conjugate. *B*, Cells were reconstructed, and drawings were overlain on the labeled barreloid.

range (7–15 mm). As illustrated by the dendrograms of Figure 6, neurons increase dendritic length by increasing the number of branches rather than the length of branches. There is a trend for cells located dorsally in the barreloids to form more elaborate trees (Fig. 6*C*); the closer a cell to the VPM/posterior group (Po) border, the larger the total length of its dendrites ($r = -0.68$; $p < 0.001$). Likewise, the proportion of extrabarreloid dendrites tends to increase with the cell proximity to Po ($r = -0.63$; $p < 0.05$) (Fig. 6*D*).

Extrabarreloid dendrites receive contacts from corticothalamic and reticular thalamic axons

Using the material shown in Figure 7, intrabarreloid and extrabarreloid dendrites were identified and examined at the EM level. The profiles forming synaptic contacts were classified into three types according to the criteria of Ralston et al. (1988). RL-type profiles (round vesicles and large terminals) are large terminals 2–4 μm in diameter containing round vesicles and pale mitochondria. They arise from lemniscal axons and form asymmetric synaptic contacts at multiple release sites (Spacek and Lieberman, 1974; McAllister and Wells, 1981; Williams et al., 1994); RS-type profiles (round vesicles and small terminals) are small terminal profiles 0.2–0.5 μm in diameter containing round vesicles and few mitochondria. They arise principally from the cerebral cortex and form asymmetric synaptic contacts (Mineff and Weinberg, 2000). F-type profiles (flattened vesicles) are terminal profiles 1–3 μm in diameter containing flattened and pleomorphic vesicles. They arise from the thalamic reticular nucleus and form symmetric synaptic contacts (Ohara and Lieberman, 1993).

Within the barreloid, 103 synaptic contacts were examined on labeled dendrites (Fig. 8*D–F*). A total of 10 RL-type profiles were found presynaptic to large proximal and medium-sized distal dendrites, 82 RS-type profiles were found presynaptic to medium- and small-sized distal dendrites, and 11 F-type profiles were found presynaptic to dendrites of all sizes. On extrabarreloid dendrites no RL-type profile was recovered, but 126 RS-type and 3 F-type contacts were found (Fig. 8*B,C*).

DISCUSSION

The present results agree with those of Ohara and Havton (1994) on the dimension of the dendritic arbors of relay cells, their stereotyped bushy architecture, the range of total dendritic lengths, and the nontapering of distal dendrites. They also agree with results reported by Chiaia et al. (1991), particularly concerning the diversity in the orientations of the dendritic arbors. In addition, our results provide direct evidence for the spread of dendritic arbors of VPM cells in surrounding barreloids, a long suspected feature with significant functional consequences.

Thalamic barreloids only receive three main types of input: an ascending excitatory input from the principal trigeminal nucleus (PR5), an excitatory corticothalamic input from the barrel field, and an inhibitory input from the reticular thalamic nucleus. At a unitary level, these pathways are composed of axons with terminal fields restricted to the barreloid representing the principal whisker of their receptive field (Williams et al., 1994; Bourassa et al., 1995; Veinante and Deschênes, 1999; Désîlets-Roy et al., 2002). If VPM cells had dendrites confined to their home barreloid, they would function like parallel processors in closed loop connections with their corticothalamic and reticular thalamic partners. For a number of cells, extrabarreloid dendrites represent a sizeable proportion of the total dendritic arborization, which is what endows them with cross-whisker integrative functions. Thus, for most barreloid cells one can define three functional dendritic domains: (1) a principal-whisker afferent domain consisting of proximal and second-order intrabarreloid dendrites that receive contacts from PR5 axons; (2) a principal-whisker recurrent domain made of intrabarreloid dendrites that receive contacts from reticular thalamic and corticothalamic cells with principal-whisker receptive fields located on the same vibrissa; and (3) surrounding-whisker recurrent domains consisting of extrabarreloid distal dendrites that receive contacts from reticular thalamic and corticothalamic cells with principal-whisker receptive fields located on adjacent whiskers. These morphofunctional divisions emphasize the whisker-specific ordering of synaptic contacts on VPM relay cells and provide a framework to study cross-whisker interactions that still remain largely unexplored (but see Simons and Carvell, 1989).

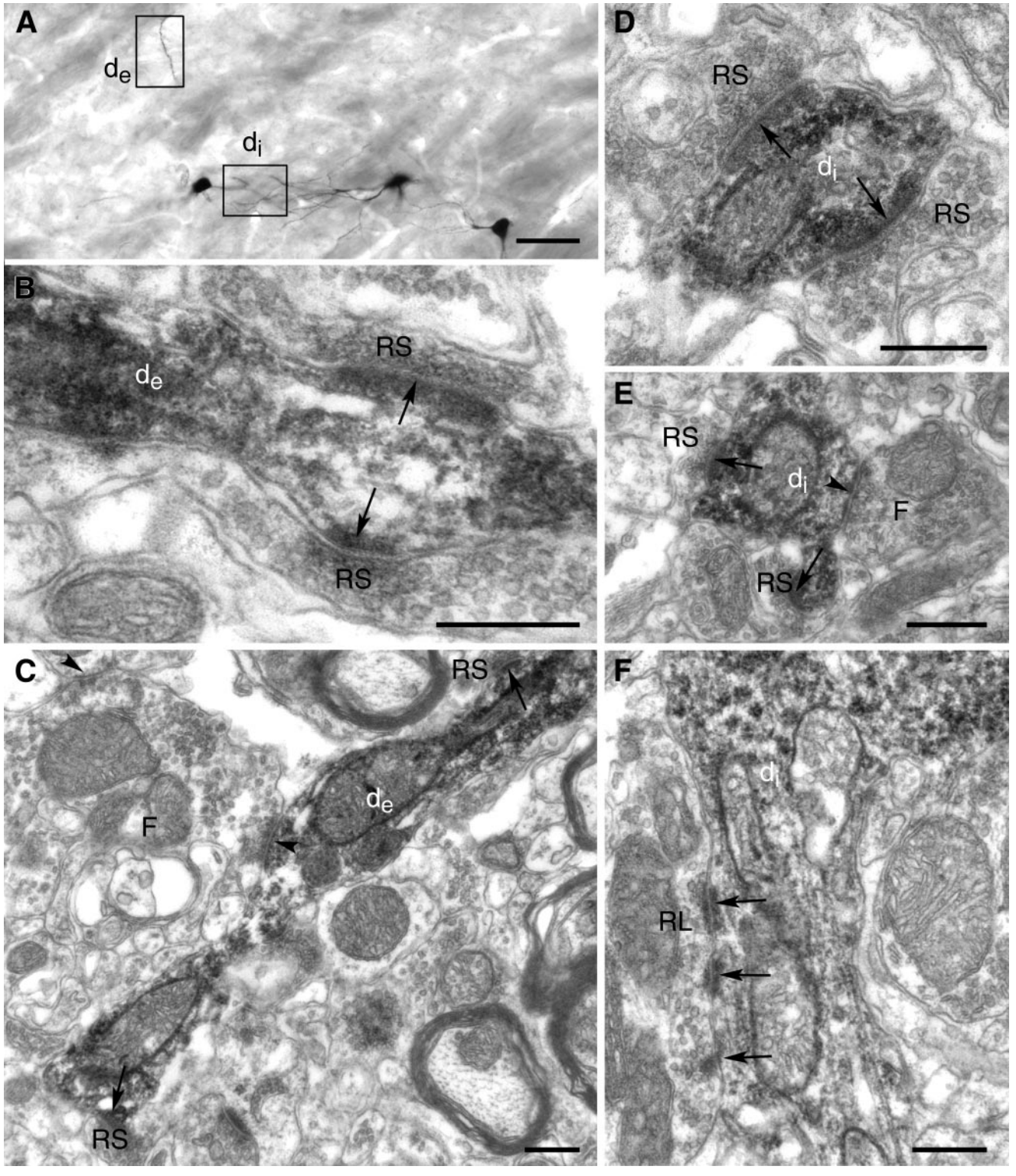

Figure 8. Examples of synaptic contacts observed on intrabarreloid and extrabarreloid dendrites of VPM cells. *A*, The three labeled cells in Figure 6 are shown after osmification and plastic embedding; *boxed areas* indicate the regions examined at the EM level. d_e, extrabarreloid dendrite; d_i, intrabarreloid dendrite. *B, C*, Examples of RS-type and F-type profiles on extrabarreloid dendrites. *D–F*, Examples of RS-type, F-type, and RL-type profiles on intrabarreloid dendrites. *Arrows* and *arrowheads* indicate asymmetrical (excitatory) and symmetrical (inhibitory) synaptic contacts, respectively. Scale bars: *A*, 50 μm; *B–F*, 0.3 μm.

Substrate for functional diversity in thalamic barreloids

On the basis of the numerical density of cells in the rat VPM, it was estimated that barreloids representing the large caudal vibrissae contain 250–300 relay cells (Land et al., 1995). This figure was considered to be an upper estimate, because the volume of barreloids was approximated by assuming that their shape conforms to that of uniform cylinders. Whatever the actual number, say ~200, the issue boils down to the question of what is mapped

across the dimensions of a barreloid. Each vibrissa is innervated by first-order afferents that respond to the magnitude and/or velocity of deflections in a direction-selective manner (Zucker and Welker, 1969; Gibson and Welker, 1983a,b; Lichtenstein et al., 1990; Shoykhet et al., 2000). Primary afferents can also be classified as on/off direction-selective on the basis of their preferential sensitivity to the onset or offset of whisker motion. Physiological studies of vibrissa-responsive units in the brainstem, thalamus, and cortex have reported the presence of units with response properties that recapitulate to various degrees the specialization found at the peripheral level (for review, see Simons, 1995). Whether these response properties define parallel channels of vibrissal information is not yet clear, and we still ignore how these properties relate to structural features such as cell location, morphology, and connections among whisker-related modules. For the moment, there is a general consensus that the rat VPM contains a single morphological type of cells that differs in the complexity and orientation of dendritic arbors. Thus, these two features should be considered as the morphological substrate of the functional specialization of the relay cells.

Our data show that cells in the dorsalmost segment of the barreloids have larger dendritic surface areas and may thus receive a larger number of synaptic contacts. This is in keeping with the fact that this region receives input from two types of PR5 cells: cells with narrow dendritic fields that form small clusters of terminals in a single barreloid and large cells with extensive dendritic fields that innervate multiple barreloids (Veinante and Deschênes, 1999). This region also receives a selective innervation from the thalamic reticular nucleus (Désîlets-Roy et al., 2002) and contains a larger number of labeled cells after retrograde tracer injection in layer 6 of the barrel field (Land et al., 1995). No physiological study has yet reported distinct response properties for cells located dorsally in barreloids, but their morphology and synaptic inputs suggest a parallel stream of vibrissal information.

In addition to the existence of parallel channels, the number of cells per barreloid may relate to the number of coactivation patterns that can be formed among adjacent whiskers. Together, cells within a barreloid do not demonstrate a preferential distribution of their dendritic arbors across rows or arcs of vibrissa representation (see also Chiaia et al., 1991). All combinatorial patterns of distribution in surrounding barreloids seem present. If the cell number is commensurate with the number of possible combinations, one would expect barreloids representing whiskers at the border of the pad to contain a smaller number of cells. In line with this contention, it was reported recently that barreloids representing row A and straddler whiskers are of smaller size than those representing whiskers located at the center of the pad (Haidarliu and Ahissar, 2001).

Structure/function relationship

The question of whether dendritic field orientation along barreloid rows and arcs is related to differences in cell response properties remains, as yet, unresolved. Under the anesthetic conditions of our experiments, most VPM cells responded to the deflection of a single whisker, which precludes any correlation to be drawn between cell morphology, response properties, and receptive field characteristics. From a strict anatomical viewpoint, however, the crossing over of dendrites in surrounding barreloids provides a substrate for cross-whisker feedback modulation of lemniscal inputs by reticular and corticothalamic axons, and the diversity of dendritic field orientations will determine the spatial pattern of recurrent modulatory actions. Because vibrissa-evoked responses in most relay cells are direction sensitive (Simons and Carvell, 1989; Lee et al., 1994), it seems plausible that maximal cross-whisker modulation will occur when a pair or a small group of whiskers is deflected in the preferred direction of the cell. Thus, the way single cells distribute dendrites across rows and arcs of barreloids might relate to the direction selectivity of their excitatory and/or inhibitory responses.

Synthesis of multiwhisker receptive fields

It is well established that in lightly anesthetized animals most VPM cells have receptive fields composed of one principal and several surrounding whiskers (Freidberg et al., 1999). For a time it was considered that afferents from the interpolaris nucleus might mediate surrounding whisker responsiveness, because receptive field sizes were significantly reduced after lesion of this nucleus (Rhoades et al., 1987; Lee et al., 1994). Tract tracing studies, however, convincingly demonstrated that PR5 and interpolaris axons innervate different territories of the VPM (Williams et al., 1994; Pierret et al., 2000). The possibility remained that, despite the point-to-point connections between PR5 barrelettes and barreloids, surrounding receptive fields result from the convergence of PR5 axons on relay cell dendrites. Our EM data do not support this hypothesis, because no lemniscal (RL-type) synaptic profiles were observed on extrabarreloid dendrites. In addition, the dendritic field span of relay cells in adjacent barreloids does not match the size of the surrounding receptive fields that comprise approximately six whiskers in lightly anesthetized animals (Freidberg et al., 1999). Although negative evidence is no proof, it seems more likely that multiwhisker receptive field synthesis occurs within the PR5 itself. Indeed, a recent study reported that in fentanyl-sedated rats most PR5 units have multiwhisker receptive fields (Minnery and Simons, 2001). The origin of surrounding whisker responses of PR5 neurons is not yet determined, but intersubnuclear pathways within the brainstem trigeminal complex might be involved (Jacquin et al., 1990). This possibility would be in line with the reduction of receptive field size of VPM cells after lesion of the interpolaris nucleus.

REFERENCES

Bourassa J, Pinault D, Deschênes M (1995) Corticothalamic projections from the cortical barrel field in rats: a single fiber study using biocytin as an anterograde tracer. Eur J Neurosci 7:19–30.

Chiaia NL, Rhoades RW, Fish SE, Killackey HP (1991) Thalamic processing of vibrissal information in the rat. II. Morphological and functional properties of medial ventral posterior nucleus and posterior nucleus neurons. J Comp Neurol 314:217–236.

Cox C, Huguenard JR, Prince DA (1996) Heterogeneous axonal arborizations of rat thalamic reticular neurons in the ventrobasal nucleus. J Comp Neurol 366:416–430.

Désîlets-Roy B, Varga C, Lavallée P, Deschênes M (2002) Substrate for cross-talk inhibition between thalamic barreloids. J Neurosci 22: RC218:1–4.

Freidberg MH, Lee SM, Ebner FF (1999) Modulation of receptive field properties of thalamic somatosensory neurons by the depth of anesthesia. J Neurophysiol 81:2243–2252.

Gibson JM, Welker WI (1983a) Quantitative studies of stimulus coding in first-order vibrissa afferents of rats. 1. Receptive field properties and threshold distributions. Somatosens Res 1:51–67.

Gibson JM, Welker WI (1983b) Quantitative studies of stimulus coding in first-order vibrissa afferents of rats. 2. Adaptation and coding of stimulus parameters. Somatosens Res 1:95–117.

Haidarliu S, Ahissar E (2001) Size gradients of barreloids in the rat thalamus. J Comp Neurol 429:372–387.

Harris RM (1986) Morphology of physiologically identified thalamocortical relay neurons in the rat ventrobasal thalamus. J Comp Neurol 251:491–505.

Hoogland PV, Welker E, Van der Loos H (1987) Organization of the projections from barrel cortex to thalamus in mice studied with *Phaseolus vulgaris-leucoagglutinin* and HRP. Exp Brain Res 68:73–87.

Jacquin MF, Chiaia NL, Haring JH, Rhoades RW (1990) Intersub-

nuclear connections within the rat trigeminal brainstem complex. Somatosens Mot Res 7:399–420.
Land PW, Buffer SA, Yaskosky DJ (1995) Barreloids in adult rat thalamus: three-dimensional architecture and relationship to somatosensory cortical barrels. J Comp Neurol 355:573–588.
Lee SM, Friedberg MH, Ebner FF (1994) The role of GABA-mediated inhibition in the rat ventral posterior medial thalamus. I. Assessment of receptive field changes following thalamic reticular nucleus lesions. J Neurophysiol 71:1702–1713.
Lichtenstein SH, Carvell CA, Simons DJ (1990) Responses of rat trigeminal ganglion neurons to movements of vibrissae in different directions. Somatosens Mot Res 7:47–75.
McAllister JP, Wells J (1981) The structural organization of the ventral posterolateral nucleus in the rat. J Comp Neurol 197:271–301.
Mineff EM, Weinberg RJ (2000) Differential synaptic distribution of AMPA receptor subunits in the ventral posterior and reticular thalamic nuclei of the rat. Neuroscience 101:969–982.
Minnery BS, Simons DJ (2001) Trigeminothalamic response transformations in the rat whisker-barrel system. Soc Neurosci Abstr 27:51.12.
Ohara PT, Havton LA (1994) Dendritic architecture of rat somatosensory thalamocortical projection neurons. J Comp Neurol 341:159–171.
Ohara PT, Lieberman AR (1993) Some aspects of the synaptic circuitry underlying inhibition in the ventrobasal thalamus. J Neurocytol 9:815–825.
Pierret T, Lavallée P, Deschênes M (2000) Parallel streams for the relay of vibrissal information through thalamic barreloids. J Neurosci 20:7455–7462.
Pinault D (1996) A novel single-cell staining procedure performed *in vivo* under electrophysiological control: morpho-functional features of juxtacellularly labeled thalamic cells and other central neurons with biocytin or neurobiotin. J Neurosci Methods 65:113–136.
Ralston III HJ, Ohara PT, Ralston DD, Chazal G (1988) The neuronal and synaptic organization of the cat and primate somatosensory thalamus. In: Somatosensory integration in the thalamus (Macchi G, Rustioni A, Spreafico R, eds), pp 127–141. Amsterdam: Elsevier.
Rhoades RW, Belford GR, Killackey HP (1987) Receptive field properties of rat VPM neurons before and after selective kainic acid lesions of the trigeminal brainstem complex. J Neurophysiol 57:1577–1600.
Shoykhet M, Doherty D, Simons DJ (2000) Coding of deflection velocity and amplitude by whisker primary afferent neurons: implications for higher level processing. Somatosens Mot Res 17:171–180.
Simons DJ (1995) Neuronal integration in the somatosensory whisker/barrel cortex. In: Cerebral cortex, Vol 12: the barrel cortex of rodents (Jones EG, Diamond IT, eds), pp 263–297. New York: Plenum.
Simons DJ, Carvell GE (1989) Thalamocortical response transformation in the rat vibrissa/barrel system. J Neurophysiol 61:311–330.
Spacek J, Lieberman AR (1974) Ultrastructure and three-dimensional organization of synaptic glomeruli in rat somatosensory thalamus. J Anat 117:487–516.
Van der Loos H (1976) Barreloids in the mouse somatosensory thalamus. Neurosci Lett 2:1–6.
Veinante P, Deschênes M (1999) Single- and multi-whisker channels in the ascending projections from the principal trigeminal nucleus in the rat. J Neurosci 19:5085–5095.
Williams MN, Zahm DS, Jacquin MF (1994) Differential foci and synaptic organization of the principal and spinal trigeminal projections to the thalamus in the rat. Eur J Neurosci 6:429–453.
Woolsey TA, Van der Loos H (1970) The structural organization of layer IV in the somatosensory region (S1) of mouse cerebral cortex: the description of a cortical field composed of discrete cytoarchitectonic units. Brain Res 17:205–242.
Zantua JB, Wasserstrom JP, Arends JJ, Jacquin MF, Woolsey TA (1996) Postnatal development of mouse "whisker" thalamus: ventroposterior medial nucleus (VPM), barreloids, and their thalamocortical relay cells. Somatosens Mot Res 13:307–322.
Zucker E, Welker WL (1969) Coding of somatic sensory input by vibrissae neurons in the rat's trigeminal ganglion. Brain Res 12:138–156.